

Available online at [www.sciencedirect.com](http://www.sciencedirect.com)

ScienceDirect

[www.elsevier.com/locate/jes](http://www.elsevier.com/locate/jes)

JES

JOURNAL OF  
ENVIRONMENTAL  
SCIENCES[www.jesc.ac.cn](http://www.jesc.ac.cn)

# Synthesis of zinc-carboxylate metal-organic frameworks for the removal of emerging drug contaminant (amodiaquine) from aqueous solution

Adedibu C. Tella<sup>1,\*</sup>, Samson O. Owalude<sup>1</sup>, Sunday J. Olatunji<sup>1</sup>, Vincent O. Adimula<sup>1</sup>, Sunday E. Elaigwu<sup>1</sup>, Lukman O. Alimi<sup>2</sup>, Peter A. Ajibade<sup>3</sup>, Oluwatobi S. Oluwafemi<sup>4,5,\*</sup>

1. Department of Chemistry, University of Ilorin, P.M.B.1515 Ilorin, Nigeria

2. Department of Chemistry and Polymer Science, Stellenbosch University, 7602 Stellenbosch, Western Cape, South Africa

3. School of Chemistry and Physics, University of KwaZulu-Natal, Scottsville 3209, South Africa

4. Department of Applied Chemistry, University of Johannesburg, Doornfontein Campus, Doornfontein, 2028 Johannesburg, South Africa

5. Centre for Nanomaterials Science Research, University of Johannesburg, Johannesburg, South Africa

## ARTICLE INFO

### Article history:

Received 23 January 2017

Revised 2 June 2017

Accepted 13 June 2017

Available online 27 June 2017

### Keywords:

Adsorption

Metal-organic frameworks

Amodiaquine

Wastewater

## ABSTRACT

We herein report the removal of amodiaquine, an emerging drug contaminant from aqueous solution using  $[\text{Zn}_2(\text{fum})_2(\text{bpy})]$  and  $[\text{Zn}_4\text{O}(\text{bdc})_3]$  (fum = fumaric acid; bpy = 4,4-bipyridine; bdc = benzene-1,4-dicarboxylate) metal-organic frameworks (MOFs) as adsorbents. The adsorbents were characterized by elemental analysis, Fourier transform infrared (FT-IR) spectroscopy, and powder X-ray diffraction (PXRD). Adsorption process for both adsorbents were found to follow the pseudo-first-order kinetics, and the adsorption equilibrium data fitted best into the Freundlich isotherm with the  $R^2$  values of 0.973 and 0.993 obtained for  $[\text{Zn}_2(\text{fum})_2(\text{bpy})]$  and  $[\text{Zn}_4\text{O}(\text{bdc})_3]$  respectively. The maximum adsorption capacities for amodiaquine in this study were found to be 0.478 and 47.62 mg/g on the  $[\text{Zn}_2(\text{fum})_2(\text{bpy})]$  and  $[\text{Zn}_4\text{O}(\text{bdc})_3]$  MOFs respectively, and were obtained at pH of 4.3 for both adsorbents. FT-IR spectroscopy analysis of the MOFs after the adsorption process showed the presence of the drug. The results of the study showed that the prepared MOFs could be used for the removal of amodiaquine from wastewater.

© 2017 The Research Center for Eco-Environmental Sciences, Chinese Academy of Sciences.

Published by Elsevier B.V.

## Introduction

Increased applications of pharmaceuticals and personal care products (PPCPs) in various activities of man over the past decades has resulted in the occurrence of high levels of these products in wastewater thereby increasing the spate of contamination of water bodies by these products and their attendant health risk (Wolfová et al., 2013). Primarily, PPCPs reach the environment either as excreted product of human

and animal metabolism or in effluents released by pharmacies, hospitals, and manufacturing industries. Residual concentrations of these chemicals have been reported to be present in industrial effluents discharged into the environment, thereby finding their way into water bodies (Huang et al., 2011; Nikolaou et al., 2007). The development and efficiency of pharmaceutical products for the treatment of various diseases such as malaria has made them almost indispensable to man.

\* Corresponding authors. E-mails: [ac\\_tella@yahoo.co.uk](mailto:ac_tella@yahoo.co.uk) (Adedibu C. Tella), [oluwafemi.oluwatobi@gmail.com](mailto:oluwafemi.oluwatobi@gmail.com) (Oluwatobi S. Oluwafemi).

Malaria is known to be a global burden due to the fact that it affects and kills about 800,000 people annually and puts at risk about 3.3 billion people (Korenromp et al., 2013). Malaria is a disease transmitted by infected mosquitoes via the strains of malaria parasites (*Plasmodium falciparum*, *Plasmodium vivax*, *Plasmodium ovale*, *Plasmodium malariae* and *Plasmodium knowlesi*). The *P. falciparum* strain is known to be most prevalent of the 5 strains, causing severe malaria which is the most frequent cause of death for children under five years of age in Sub-Saharan Africa and about 91% of the annual deaths (Korenromp et al., 2013). Resistance of the *P. falciparum* to the common anti-malarial drugs like sulphadoxine/pyrimethamine (which is an antimalarial drug that has the sulphonamide antibiotic effect and the antiprotozoan effect of pyrimethamine), chloroquine, and amodiaquine (which is a phenyl substituted analogue of chloroquine), posed a major challenge to the fight against the prevalence of the malaria disease in Africa (Koram et al., 2005). In order to address this problem, the World Health Organization (WHO) recommended the artemisinin-based combination therapy (ACT) to combat the emergence and spread of drug-resistant uncomplicated malaria (Koram et al., 2008; Fehintola et al., 2011). One of such ACT drugs recommended was Amodiaquine/Artesunate (Hodel et al., 2010; Kopel et al., 2012).

Amodiaquine (4-((7-chloroquinolin-4-yl)amino)-2-((diethylamino)methyl)phenol) shown in Fig. 1, has been used widely for the prevention and treatment of malaria, and other conditions of arthritis (Wittes, 1987; Karunajeewa, 2015). It is an analogue of chloroquine (a phenyl substituted analogue) found to be effective against some strains of *P. falciparum*, and also a member of the 4-aminoquinolines which were considered as most important antimalarial drugs for several decades. As a result, it is commonly found in wastewater as well as drinking water. Thus, its removal is necessary to eliminate its contamination of water.

Several strategies have been proposed for the removal of PPCPs from wastewater. These strategies include photo-transformation (Ereira et al., 2007), membrane nanofiltration (Koyuncu et al., 2008), sedimentation, chlorination (Boyd et al., 2003, 2005), precipitation, adsorption (Marin et al., 2010; Li et al., 2011; Zhang et al., 2012), and ozonation (Ernes et al., 2003). The adsorption process has been proven to be very effective due its advantages over other techniques, which includes low cost, excellent removal efficiency and its applicability over a large range of adsorbent and adsorbate

concentrations (Bajpai et al., 2014). Therefore, the development of adsorbent materials, which will be efficient for the removal of emerging contaminants such as PPCPs from wastewater, is very important (Huang et al., 2011). Among the various adsorbents, such as mesoporous silica, zeolites, metal-organic frameworks (MOFs), biomaterials and activated carbon commonly used for adsorptive removal, and separation and purification of contaminants, MOFs have intrinsic characteristics that make them unique and different from the other adsorbents.

The application of MOFs in the removal of PPCPs was first reported by Jhung and co-workers (Hasan et al., 2012). The liquid-phase adsorption of naproxen and clofibric acid as representative of PPCPs were carried out using two MOFs iron-benzenetricarboxylate (MIL-100-Fe) and chromium-benzenedicarboxylate (MIL-101) and their adsorption rate and adsorption capacities were compared to those of activated carbon. The removal efficiency was reported to decrease in the order of MIL-101 > MIL-100-Fe > activated carbon in both parameters. The fast adsorption rate of MIL-101 was explained in terms of its larger pore size. The adsorption process was more favorable at lower solution pH on MIL-101 and the adsorption mechanism was therefore interpreted as simple electrostatic interaction between the PPCPs and MIL-101. This pioneer study suggested that MOF type materials could be applied in the adsorptive removal of PPCPs in contaminated water. Several other reports on the removal of PPCPs using MOFs and MOF derivatives have been well documented (Seo et al., 2016, 2017; Ahmed et al., 2017; Bhadra et al., 2017).

The structures of metal-organic frameworks (MOFs) consist of metal ions and organic ligands linked together via coordination bonds (Fan and Yan, 2012). They possess permanent porosity and have unique properties such as large surface areas (1000–10,400 m<sup>2</sup>/g), high thermal stability with tunable polarity and nanoscale pore sizes (Yaghi et al., 2003; Rowsell and Yaghi, 2004). MOFs have therefore been variously applied in catalysis (Corma et al., 2010), separation (Li et al., 2012; Xie et al., 2011), gas storage (Getman et al., 2011), drug delivery (Taylor-Pashow et al., 2009) and more importantly as adsorbents (Tella and Owalude, 2014).

Many metal-organic frameworks have been synthesized by solvent-based solvothermal and reflux techniques at temperatures between 25 to approximately 220°C. In the recent past, a number of functional metal-organic framework materials have been reported based on these techniques. A metal-organic framework material constructed from Zn(II) and the ligand 2,5-di(3',5'-dicarboxylphenyl)pyridine has been reported (Liu et al., 2016a). The compound was demonstrated to possess the ability to selectively sense nitrobenzene and therefore can be employed in detection of explosives. The study also showed that the metal-organic framework materials displayed multifarious applications for selective adsorption of Fe<sup>3+</sup> ions and dyes and their subsequent separation from solutions. A metal-organic framework based on the ligand 5-nitroisophthalate and co-ligand 2,2'-dimethyl-4,4'-bipyridine has also been reported (Ma et al., 2015). These ligands were functionalized by incorporating hydrophobic functional groups, such as, methyl and nitril in their structures. The resulting MOF is hydrostable with a 3D dia topology and highly selective in busulfan payloads. High

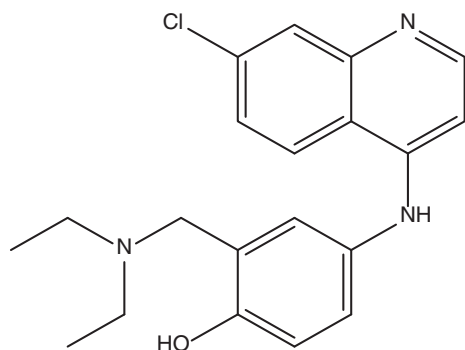


Fig. 1 – Chemical structure of amodiaquine.

encapsulation efficiency of 21.5% with a 100% progressive release of the drug was reported to occur within 36 hr. Molecular simulations were performed and the results revealed that the MOF has a very high adsorption for CO<sub>2</sub>.

A new high thermally stable metal–organic framework (GDMU-2) was designed by employing a ligand functionalization technique (Liu et al., 2016b). The MOF was prepared by the incorporation of Cu into a functionalized trigonal tri-isophthalate ligand (3,3',3'',5,5',5''-pyridyl-1,3,5-triylhexabenzic acid) under solvothermal condition. The resulting gdm-MOF has open copper sites well aligned the cub-octahedron with high hydrogen storage capacity of 240.7 cm<sup>3</sup>/gat 77 K and 1 bar. Liu and co-workers also reported a new class of MOFs constructed from the reaction of the ligands 2,6-di(3',5'-dicarboxylphenyl)pyridine and 2,5-di(3',5'-dicarboxylphenyl)pyridine with hydrated metal nitrates of copper, zinc and samarium (Liu et al., 2015). The three MOFs were demonstrated to have high capacities to adsorb large amounts of the drug 5-fluorouracil (5-FU) and with a progressive release in each case. Grand Canonical Monte Carlo (GCMC) simulations revealed that the calculated drug load is more related to the molecular properties of accessible volume ( $V_{acc}$ ) than to the pore sizes of the respective MOFs. A microporous metal–organic framework (JLU-Liu1) prepared by the solvothermal reaction of 4-(pyrimidin-5-yl) benzoic acid with hydrated copper(II) sulfate in N,N-dimethylformamide (DMF) at 115°C for 24 hr has been reported (Luo et al., 2013). The MOF has a unique octa-nuclear copper clusters with highly selective CO<sub>2</sub> uptake over N<sub>2</sub> and CH<sub>4</sub> when activated. The MOF could therefore be a good candidate for separation of a mixture containing CO<sub>2</sub> and CH<sub>4</sub>.

A review on the application of metal–organic frameworks as solid-phase sorbents (SPSs) has been reported by Wen et al. (2014). These applications include the use of MOFs as chromatographic solid phases in the separations of linear and branched alkanes, as well as aromatic positional isomers. Some MOFs based on a bipyridinium ligand were also applied in GC for the separation of alcohol-water mixtures. Other SPS applications of MOFs in the review range from coupling with high-performance liquid chromatography (HPLC) for determination of polycyclic aromatic hydrocarbons in environmental waters; fabrication in a polyetheretherketone (PEEK) tube as micro-trapping device and adsorptive extraction of naproxen and its metabolite in urine samples. Metal–organic framework ([MIL-101]) was magnetized by coating with magnetic Fe<sub>3</sub>O<sub>4</sub> microspheres and applied as magnetic solid-phase extraction (MSPE) adsorbents for preconcentration of four kinds of pyrazole/pyrrole pesticides in environmental water samples (Ma et al., 2016). The magnetized MOF was coupled with HPLC-DAD (diode-array detector) for determination of these pollutants. Under optimized conditions, the developed MOF was convenient, rapid and eco-friendly in the sensitive determination of pyrazole/pyrrole pesticides with high reusability and also demonstrated excellent practical applicability.

MOF-5 ([Zn<sub>4</sub>O(bdc)<sub>3</sub>] (bdc = benzene-1,4-dicarboxylate) is one of the most studied due to its large surface area and pore volume and therefore has been subjected to a wide varieties of applications. Friedel–Crafts benzylation of toluene with benzyl bromide has been carried out using [Zn<sub>4</sub>O(bdc)<sub>3</sub>] as a heterogeneous acid catalyst (Phan et al., 2010). The major

product (*p*-benzyltoluene) was obtained in a quantitative yield in 4 hr with 60% selectivity. A trace amount of *m*-benzyltoluene was detected as a by-product of the reaction. Other applications in catalysis have been reported for this MOF (Isaeva et al., 2008; Kleist et al., 2010; Chughtai et al., 2015). Several technologies have been developed for hydrogen storage as an ideal alternative to fossil-fuel systems and application of [Zn<sub>4</sub>O(bdc)<sub>3</sub>] in this process have been reported by several authors. Yaghi and co-workers pioneered this with [Zn<sub>4</sub>O(bdc)<sub>3</sub>] and a high hydrogen storage capacities, 4.5 wt.% at 77 K and 0.8 bar and 1 wt.% at room temperature and 20 bar was reported (Li et al., 1999). This group later reported that, the maximum hydrogen uptake of MOF-5 could reach 1.32 wt.% at 1 bar and 77 K (Rowse et al., 2004). Several other authors have successfully applied this MOF for hydrogen storage (Li et al., 2009).

The disposal of solvents used in chemical reactions present a lot of environmental problems; synthetic chemists have therefore been looking for alternative and more environmental friendly preparative approach (Tella et al., 2014; Tella and Owalude, 2014). In this paper, we have adopted a solid state approach to the preparation of known MOFs [Zn<sub>2</sub>(fum)<sub>2</sub>(bpy)] (fum = fumaric acid; bpy = 4,4-bipyridine) and [Zn<sub>4</sub>O(bdc)<sub>3</sub>]. Ability of the MOFs in the adsorption of amodiaquine (an emerging contaminant) from solution using a batch experiment was investigated. Effects of parameters such as initial concentration, contact time, temperature, pH, and adsorbent dosage on the adsorption process were also determined. The adsorption data were analyzed using suitable equilibrium adsorption isotherms.

## 1. Experimental

### 1.1. Materials and methods

Zinc nitrate hexahydrate (99%), zinc acetate dihydrate (99%), terephthalic acid (bdc, 99%), fumaric acid (fum, 99%) and 4, 4'-bipyridine (bpy, 98%) were obtained from British Drug Houses (BDH) Chemicals Ltd., England; Aldrich Chem., Germany; and Junsei Chem. Co. Ltd., Japan. N,N-dimethylformamide (DMF, 99%) was obtained from Aldrich Chem., Germany, and amodiaquine (92%) was obtained from Tuyil Pharmaceutical Industry, Ilorin, Nigeria. All chemicals were used as purchased.

### 1.2. Synthesis of [Zn<sub>2</sub>(fum)<sub>2</sub>(bpy)]MOF

[Zn<sub>2</sub>(fum)<sub>2</sub>(bpy)] MOF was synthesized by following a literature procedure (Tella and Owalude, 2014). Fumaric acid (0.232 g, 2 mmol), 4, 4-bipyridine (0.156 g, 1 mmol), and Zinc acetate dihydrate (0.428 g, 2 mmol) were accurately weighed into an agate mortar and grinded together continuously for 15 min to a fine powder. The white powder obtained was washed with ethanol then dried at room temperature and stored in a desiccator.

### 1.3. Synthesis of [Zn<sub>4</sub>O(bdc)<sub>3</sub>] MOF

[Zn<sub>4</sub>O(bdc)<sub>3</sub>] MOF was synthesized by adopting a procedure similar to a previously reported method (Li et al., 2009; Dikio

and Farah, 2013). Terephthalic acid (0.332 g, 2 mmol) was dissolved in 40 mL DMF and 3 mL triethylamine was added to the solution. Zinc nitrate hexahydrate (1.188 g, 4 mmol) was dissolved in 40 mL DMF and mixed with the solution of terephthalic acid under continuous stirring. The mixture was then sealed and stirred for 3 hr at room temperature. A white precipitate was obtained and filtered out of the solution. The product obtained was purified by washing with DMF. The purified  $[\text{Zn}_4\text{O}(\text{bdc})_3]$  MOF was dried for 5 hr at  $100^\circ\text{C}$  and stored in a desiccator after cooling to room temperature.

#### 1.4. Characterization of adsorbents

Elemental analysis of the synthesized adsorbents was carried out on a Perkin-Elmer CHN Analyzer 2400 series II (CHN Analyzer 2400 series II, Perkin-Elmer, USA). FTIR spectrum was recorded on a Shimadzu 8400 spectrophotometer (8400, Shimadzu, Japan) using KBr pellets. Powder X-ray diffraction (PXRD) analysis was measured on a Bruker D8 Advance X-ray diffractometer (Bruker D8, Bruker, UK) using a  $\text{CuK}\alpha$ -radiation (wavelength of monochromatic radiation,  $\lambda = 1.5406 \text{ \AA}$ ) operating at 30 kV and 40 mA.

#### 1.5. Batch adsorption studies

Prior to adsorption, the adsorbents  $[\text{Zn}_2(\text{fum})_2(\text{bpy})]$  and  $[\text{Zn}_4\text{O}(\text{bdc})_3]$  MOFs were activated via overnight drying at  $120^\circ\text{C}$  and stored in a desiccator. Adsorption of amodiaquine on  $[\text{Zn}_2(\text{fum})_2(\text{bpy})]$  and  $[\text{Zn}_4\text{O}(\text{bdc})_3]$  MOFs was studied with a stock solution of amodiaquine (200 mg/L) prepared by dissolving 200 mg of amodiaquine in 1 L of deionized water. Lower concentrations (5–30 mg/L) of the drug were obtained by successive dilution of the stock solution with deionized water. The concentration of amodiaquine was determined by measuring the absorbance of the solutions at the wavelength at which the maximum fraction of light is absorbed by the solution ( $\lambda_{\text{max}} = 340 \text{ nm}$ ) using a SHIMADZU UV-1650pc Ultraviolet-Visible (UV-Vis) spectrophotometer (SHIMADZU UV-1650pc, SHIMADZU Europe, Europe). The calibration curve was plotted from the absorbance of the prepared standard solutions of amodiaquine (5–30 mg/L). 50 mL each of the amodiaquine solutions prepared with concentrations ranging between 5 to 30 mg/L were placed in Erlenmeyer flasks. A quantity of the adsorbents (0.05 g) was weighed into each of the flasks followed by shaken in an incubator shaker at a constant speed of 165 r/min at  $30^\circ\text{C}$  for a fixed time (10 min to 12 hr). The adsorbent materials were thereafter filtered and the amodiaquine concentration in the filtrates was determined using SHIMADZU UV-1650pc UV-Vis spectrophotometer (SHIMADZU UV-1650pc, SHIMADZU Europe) at  $\lambda_{\text{max}} = 340 \text{ nm}$ . The amount of amodiaquine adsorbed onto the  $[\text{Zn}_2(\text{fum})_2(\text{bpy})]$  and  $[\text{Zn}_4\text{O}(\text{bdc})_3]$  MOFs was obtained using the expression (Bajpai et al., 2014; Elaigwu et al., 2014):

$$q_{\text{eq}} = \frac{(C_0 - C_{\text{eq}})V}{m} \quad (1)$$

where  $q_{\text{eq}}$  is the equilibrium adsorption capacity of amodiaquine adsorbed on unit mass of adsorbent (mg/g),  $C_0$  and  $C_{\text{eq}}$  are the initial and equilibrium concentrations of amodiaquine (mg/L),  $V$  is the volume of the solution of the adsorbate in liters (L), and  $m$  is the amount of adsorbent in grams (g), respectively.

## 2. Results and discussion

### 2.1. Characterization of the adsorbents

#### 2.1.1. FTIR analysis

FTIR spectra of  $[\text{Zn}_2(\text{fum})_2(\text{bpy})]$  and  $[\text{Zn}_4\text{O}(\text{bdc})_3]$  MOFs before and after adsorption of amodiaquine are shown in Fig. 2a and b, respectively. The asymmetric  $\text{COO}^-$  ( $\nu_{\text{asym}}(\text{COO}^-)$ ) and symmetric  $\text{COO}^-$  ( $\nu_{\text{sym}}(\text{COO}^-)$ ) peaks were found at  $1627$  and  $1390 \text{ cm}^{-1}$  for  $[\text{Zn}_2(\text{fum})_2(\text{bpy})]$  and  $1567$  and  $1392 \text{ cm}^{-1}$  for  $[\text{Zn}_4\text{O}(\text{bdc})_3]$ , respectively. The  $\Delta\nu$  ( $\nu_{\text{asym}} - \nu_{\text{sym}}$ ) values for the carboxylate group in  $[\text{Zn}_2(\text{fum})_2(\text{bpy})]$  and  $[\text{Zn}_4\text{O}(\text{bdc})_3]$  are  $237$  and  $175 \text{ cm}^{-1}$ , respectively which suggest monodentate for  $[\text{Zn}_2(\text{fum})_2(\text{bpy})]$  and bidentate mode of coordination for  $[\text{Zn}_4\text{O}(\text{bdc})_3]$  (Ibrahim et al., 2005; Abbasi et al., 2013).

FTIR spectra of  $[\text{Zn}_2(\text{fum})_2(\text{bpy})]$  MOF (Fig. 2a), after the adsorption of amodiaquine showed a band at  $705 \text{ cm}^{-1}$  which corresponds to the characteristic IR bands of the  $-\text{C}-\text{Cl}$  group of the adsorbate, while the FTIR spectra of the  $[\text{Zn}_4\text{O}(\text{bdc})_3]$  adsorbent (Fig. 2b), after the adsorption of amodiaquine showed a band observed at  $522 \text{ cm}^{-1}$  which corresponds to the  $-\text{C}-\text{Cl}$  group of the adsorbate (Arlinghaus and Andrews, 1984).

#### 2.1.2. PXRD analysis

The observed PXRD pattern of the  $[\text{Zn}_2(\text{fum})_2(\text{bpy})]$  MOF prepared and the simulated pattern obtained from Cambridge Structural database (CSD code MAVNUT01), and from published data (Tella and Owalude, 2014), are presented in Fig. 3. The comparison of both patterns indicated that the adsorbent is

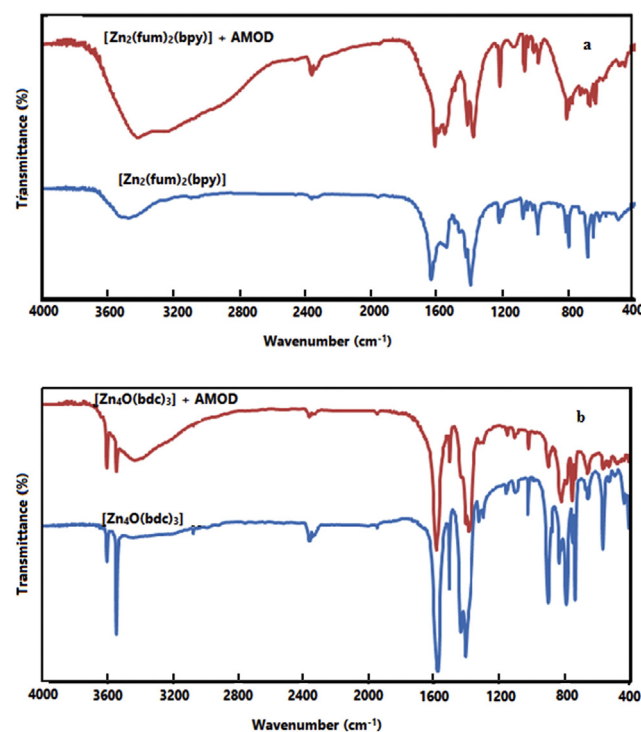
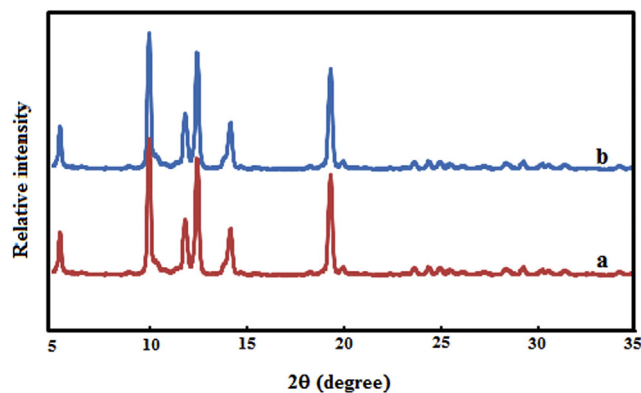


Fig. 2 – Infrared spectra of (a)  $[\text{Zn}_2(\text{fum})_2(\text{bpy})]$  and (b)  $[\text{Zn}_4\text{O}(\text{bdc})_3]$  before and after adsorption of amodiaquine (AMOD). fum: fumaric acid; bpy: 4,4-bipyridine; bdc: = benzene-1,4-dicarboxylate.



**Fig. 3** – Comparison of powder X-ray diffraction (PXRD) patterns of simulated patterns of  $[\text{Zn}_2(\text{fum})_2(\text{bpy})]$  MOFs (a) obtained from Cambridge crystallographic data centre (CCDC) and literature (Tella and Owulude, 2014) and (b) prepared. MOFs: metal–organic frameworks.

$[\text{Zn}_2(\text{fum})_2(\text{bpy})]$  MOF with both patterns showing high intensity peaks at  $9.98^\circ$ . In Fig. 4, comparison of the X-ray diffraction pattern of the prepared  $[\text{Zn}_4\text{O}(\text{bdc})_3]$  MOF and that of the simulated pattern obtained from Cambridge Structural database (CSD code SAHYIK), showed that the synthesized compound closely matched the compound synthesized via a solvothermal procedure reported by Li and co-workers (Li et al., 2009).

### 2.1.3. Elemental analysis

Comparison of the experimental results of the elemental analyses carried out on the synthesized  $[\text{Zn}_2(\text{fum})_2(\text{bpy})]$  and  $[\text{Zn}_4\text{O}(\text{bdc})_3]$  adsorbents with the calculated values shows a close match and the formation of a pure compound. The elemental analyses results are present in Table 1.

## 2.2. Adsorption studies

The adsorption ability of MOFs has been thoroughly investigated by several researchers. There are many factors that affect the adsorbability of dissolved substances. These include the chemical form of the substance, initial concentration, contact time, temperature, solution pH and adsorbent dosage.

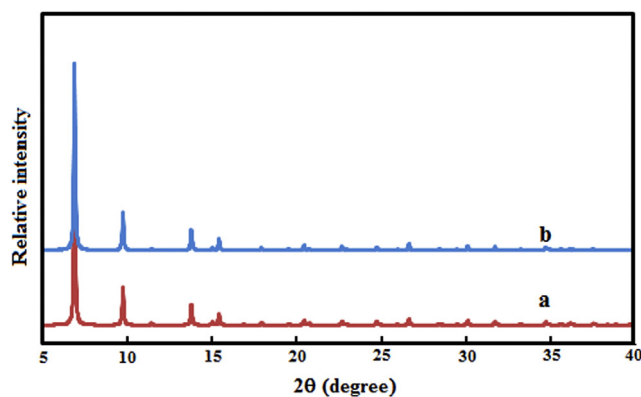


**Fig. 4** – Comparison of PXRD patterns of simulated patterns of  $[\text{Zn}_4\text{O}(\text{bdc})_3]$  MOFs (a) obtained from CCDC (Li et al., 1999) and (b) prepared.

**Table 1** – Result of the elemental analysis of  $[\text{Zn}_2(\text{fum})_2(\text{bpy})]$  and  $[\text{Zn}_4\text{O}(\text{bdc})_3]$  metal organic frameworks (MOFs).

MOFs	Elemental analysis found (calculated)		
	C	H	N
$[\text{Zn}_2(\text{fum})_2(\text{bpy})]$	41.70% (41.63%)	3.11% (3.08%)	5.43% (5.40%)
$[\text{Zn}_4\text{O}(\text{bdc})_3]$	43.27% (44.21%)	5.20% (5.02%)	7.56% (7.64%)

fum: fumaric acid; bpy: 4,4-bipyridine; bdc: benzene-1,4-dicarboxylate.

The ability of  $[\text{Zn}_2(\text{fum})_2(\text{bpy})]$  and  $[\text{Zn}_4\text{O}(\text{bdc})_3]$  to adsorb amodiaquine from aqueous at different optimized condition of concentration, time, pH and temperature was studied.

### 2.2.1. Effect of initial concentration

The effect of initial concentration of amodiaquine on the adsorption process is shown in Fig. 5. The experiment was carried out at  $30 \pm 2^\circ\text{C}$  for 240 min using adsorbate concentration of 5–30 mg/L, and 0.05 g of  $[\text{Zn}_4\text{O}(\text{bdc})_3]$  and  $[\text{Zn}_2(\text{fum})_2(\text{bpy})]$  MOFs adsorbent at pH of 6.8. Adsorption of amodiaquine on the  $[\text{Zn}_4\text{O}(\text{bdc})_3]$  and  $[\text{Zn}_2(\text{fum})_2(\text{bpy})]$  MOFs was observed to increase with increase in concentration up to 25 mg/L. The relationship between the drug concentration and the available binding sites on an adsorbent surface is a factor on which the effect of initial concentration of the adsorbate on the adsorption process depends (Kannan and Sundaram, 2001; Elaigwu et al., 2014). At low drug concentration, there are unoccupied sites for adsorption on the adsorbents, which became occupied as the concentration of the adsorbate increased. This led to the reduction in the adsorption sites thus, slowing down the adsorption process. This explains the decrease in amount of the adsorbate after the 25 mg/L concentration (Chen et al., 2011; Eren and Acar, 2006; Olgun and Atar, 2012).

### 2.2.2. Effect of contact time on amodiaquine adsorption

The result of the effect of contact time on adsorption of amodiaquine from solution by  $[\text{Zn}_2(\text{fum})_2(\text{bpy})]$  and  $[\text{Zn}_4\text{O}(\text{bdc})_3]$  MOFs is presented in Fig. 6. The experiment was carried out at  $30 \pm 2^\circ\text{C}$  with 25 mg/L solution of amodiaquine and 0.05 g of adsorbents at a pH of 6.8. The adsorption of amodiaquine on the adsorbents was studied over a contact time period of 0–720 min

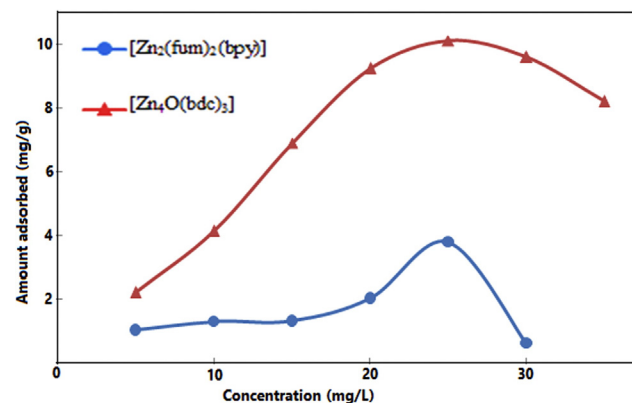


**Fig. 5** – Effect of initial concentration on the adsorption of amodiaquine on  $[\text{Zn}_4\text{O}(\text{bdc})_3]$  and  $[\text{Zn}_2(\text{fum})_2(\text{bpy})]$  MOFs at  $30 \pm 2^\circ\text{C}$ , pH 6.8, speed 165 r/min, and time 240 min.

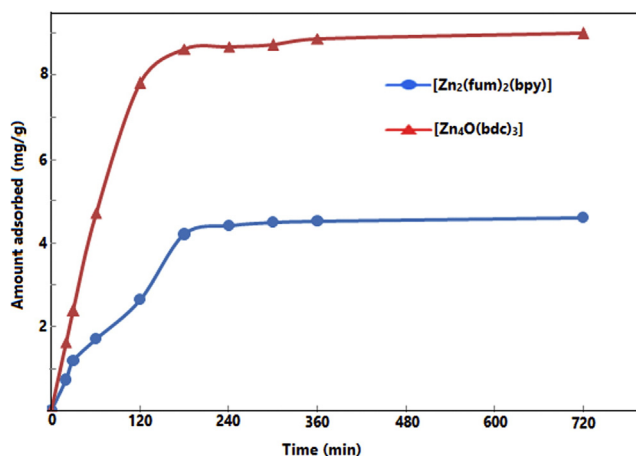


Fig. 6 – Effect of contact time on the adsorption of amodiaquine over [Zn<sub>4</sub>O(bdc)<sub>3</sub>] and [Zn<sub>2</sub>(fum)<sub>2</sub>(bpy)] MOFs at 30 ± 2°C, concentration 25 mg/L, pH 6.8, and speed 165 r/min.

in order to determine the equilibrium time of adsorption. The adsorption process was observed to increase rapidly up to 180 min and no further increase was observed thereafter. Majority of the removal occurred within 180 min which accounts for 4.20 mg/g on the [Zn<sub>2</sub>(fum)<sub>2</sub>(bpy)] MOF and 8.50 mg/g on the [Zn<sub>4</sub>O(bdc)<sub>3</sub>] MOF. The rapid increase in the amount of amodiaquine adsorbed on the adsorbents at the initial period can be attributed to the vacant adsorption sites available, which became occupied with time, thus, slowing down the adsorption process after 180 min (Cuerda-Correa et al., 2010; Chen et al., 2011). Hence, the required time for equilibrium to be attained in this study was taken as 180 min.

2.2.3. Effect of temperature on adsorption

The effect of temperature on adsorption of amodiaquine from the solution by the [Zn<sub>2</sub>(fum)<sub>2</sub>(bpy)] and [Zn<sub>4</sub>O(bdc)<sub>3</sub>] MOFs is shown in Fig. 7. The study was carried out using 25 mg/L concentration of amodiaquine and 0.05 g of adsorbents at a pH of 6.8 for 180 min, while the temperature was varied from 30 to

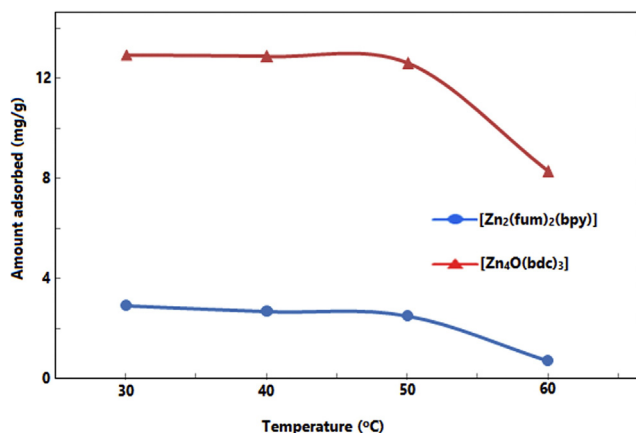


Fig. 7 – Effect of temperature on the adsorption of amodiaquine on [Zn<sub>2</sub>(fum)<sub>2</sub>(bpy)] and [Zn<sub>4</sub>O(bdc)<sub>3</sub>] MOFs. Reaction conditions: concentration 25 mg/L, pH 6.8, speed 165 r/min, and time 180 min.

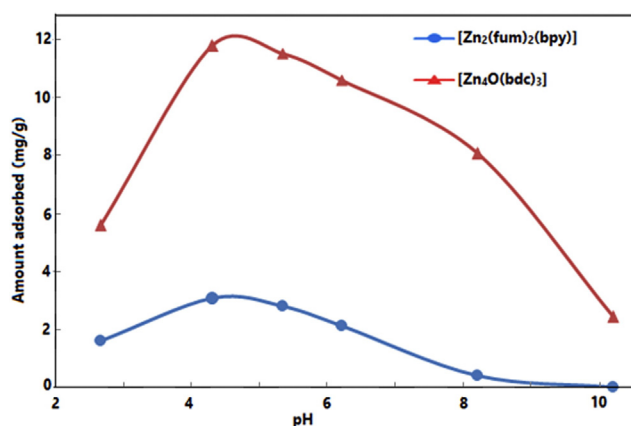


Fig. 8 – Effect of pH on the adsorption of amodiaquine on [Zn<sub>4</sub>O(bdc)<sub>3</sub>] and [Zn<sub>2</sub>(fum)<sub>2</sub>(bpy)] MOFs at 30 ± 2°C, concentration 25 mg/L, speed 165 r/min, and time 180 min.

60°C. It was observed that the amount of amodiaquine adsorbed on both adsorbents remained constant over the temperature range of 30–50°C, and then a decrease in amodiaquine adsorption were observed thereafter. The maximum uptake of 2.909 and 12.958 mg/g of amodiaquine were observed at a temperature of 30°C with [Zn<sub>4</sub>O(bdc)<sub>3</sub>] and [Zn<sub>2</sub>(fum)<sub>2</sub>(bpy)] MOFs respectively, these remained constant until a temperature of 50°C was attained. The observed trend is as a result of weak interaction between the adsorbate and adsorbent molecules due to increase in temperature (Rasheed, 2013).

2.2.4. Effect of pH on amodiaquine uptake and point of zero charge

The pH effect on the amount of amodiaquine adsorbed on the [Zn<sub>4</sub>O(bdc)<sub>3</sub>] and [Zn<sub>2</sub>(fum)<sub>2</sub>(bpy)] MOFs is shown in Fig. 8. The experiment was carried out using 25 mg/L amodiaquine concentration and 0.05 g of adsorbent for 180 min over a pH range of 2–10. Adjustment of the pH was carried out using 0.1 mol/L HCl and 0.1 mol/L NaOH. The result shows that adsorption of amodiaquine on the adsorbents increased with increasing pH. Maximum adsorption of 11.92 and 3.02 mg/g of amodiaquine on the [Zn<sub>4</sub>O(bdc)<sub>3</sub>] and [Zn<sub>2</sub>(fum)<sub>2</sub>(bpy)] MOFs respectively was observed at a pH of 4.3. Thereafter,

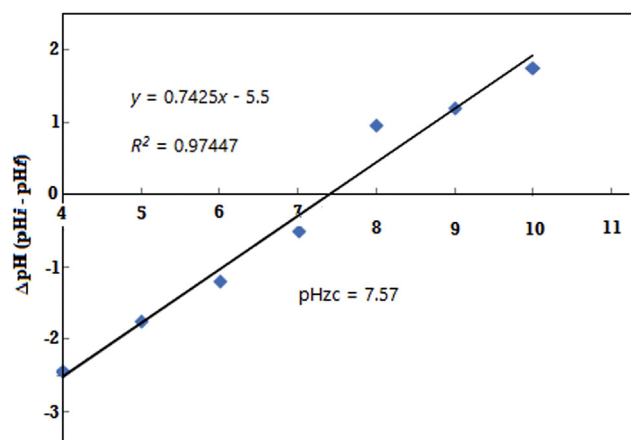


Fig. 9 – Plot of zero-point charge of [Zn<sub>4</sub>O(bdc)<sub>3</sub>]. pH<sub>zc</sub>: zero charge pH; pH<sub>i</sub>: initial pH; pH<sub>f</sub>: final pH.

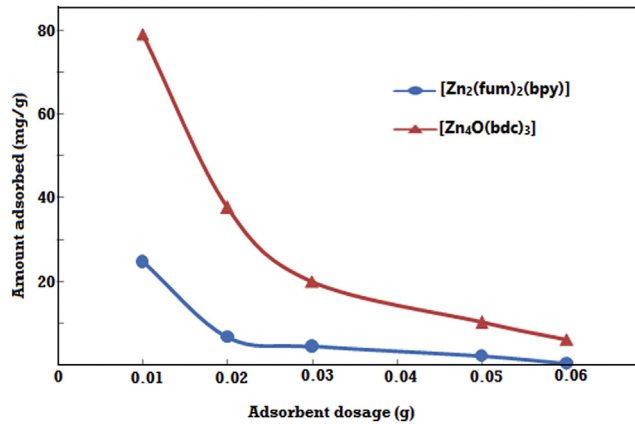


Fig. 10 – Effect of adsorbent dosage on the adsorption of amodiaquine on [Zn<sub>2</sub>(fum)<sub>2</sub>(bpy)] and [Zn<sub>4</sub>O(bdc)<sub>3</sub>] MOFs at 30 ± 2°C, concentration 25 mg/L, pH 4.3, time 180 min, and speed 165 r/min.

adsorption of amodiaquine on to the adsorbents decreased with further increase in pH of the solution.

The point of zero charge of [Zn<sub>4</sub>O(bdc)<sub>3</sub>] was determined using a literature procedure (Khan and Sarwar, 2007), the results is plotted as Fig. 9. It can be observed from the figure that the point of zero charge is at pH 7.57, a value that is higher than pH 4.3 obtained as the pH of maximum adsorption for both adsorbents. These results suggest that the surface of the adsorbents is positively charged. This proves that the adsorptions occurs between negatively charged sites in the amodiaquine anion and positively charged sites of adsorbent and thus lend further support to the electrostatic mode of adsorption proposed in this study.

#### 2.2.5. Effect of adsorbent dosage

Fig. 10 shows the effect of adsorbent dosage on the adsorption of amodiaquine on to [Zn<sub>2</sub>(fum)<sub>2</sub>(bpy)] and [Zn<sub>4</sub>O(bdc)<sub>3</sub>] MOFs. The experiment was carried out at a temperature of 30 ± 2°C using 0.01–0.06 g of adsorbent dosage and 25 mg/L of adsorbate concentration for 180 min. The result reveals that the amounts of adsorbed amodiaquine decrease rapidly with increase in the

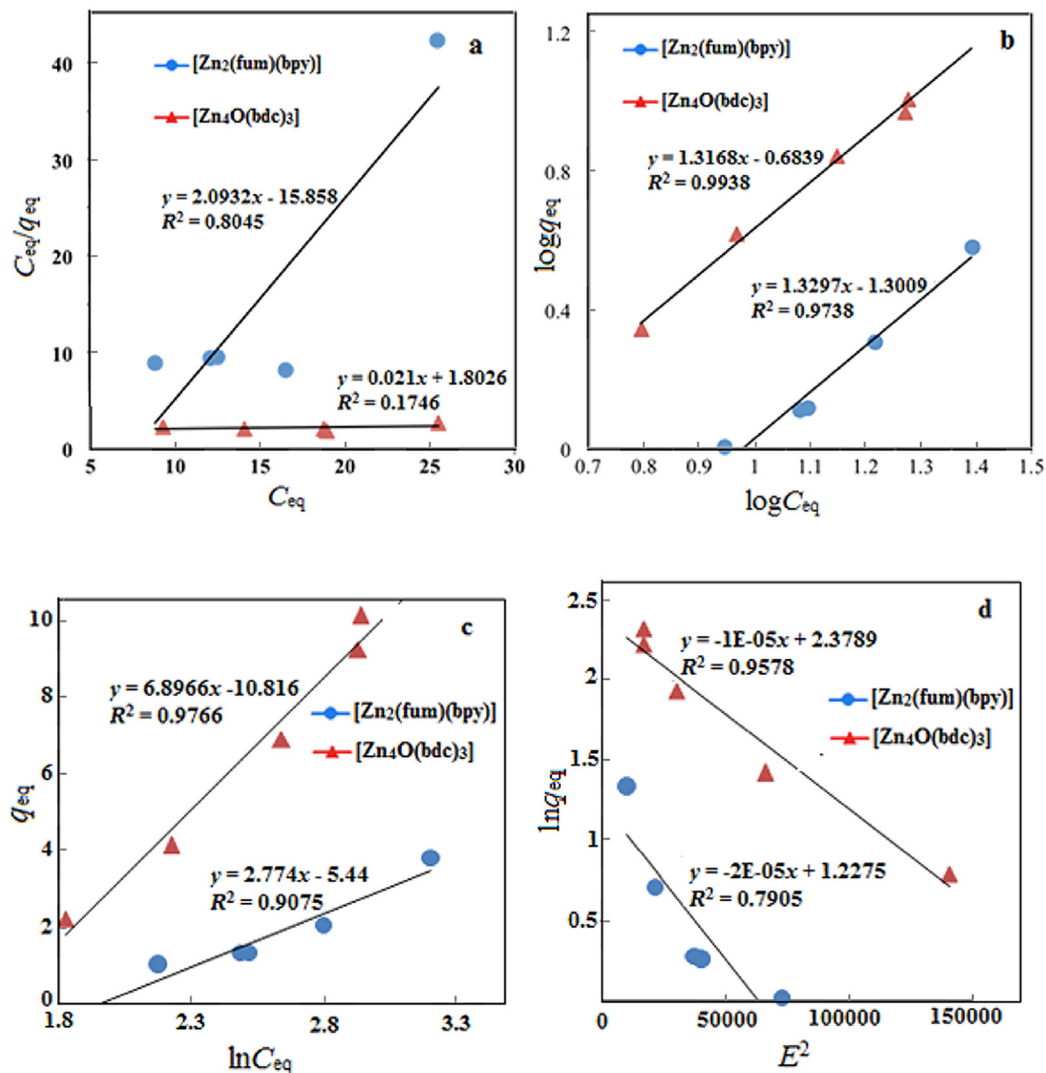


Fig. 11 – Adsorption isotherms (a) Langmuir, (b) Freundlich, (c) Temkin, and (d) Dubinin.  $q_{eq}$ : the amount adsorbed per unit mass of the adsorbent at equilibrium;  $C_{eq}$ : the equilibrium concentration of adsorbate;  $E$ : the mean free energy.

**Table 2 – Isotherm parameters for the adsorption of amodiaquine over [Zn<sub>2</sub>(fum)<sub>2</sub>(bpy)] and [Zn<sub>4</sub>O(bdc)<sub>3</sub>] at 30 ± 2°C.**

MOFs	Langmuir isotherm			Freundlich isotherm			Temkin isotherm			Dubinin–Raduskevich isotherm		
	Q <sub>max</sub> (mg/g)	K <sub>L</sub> (L/mg)	R <sup>2</sup>	K <sub>F</sub> (mg/g)	n	R <sup>2</sup>	B (J/mol)	A <sub>T</sub> (L/g)	R <sup>2</sup>	q <sub>s</sub>	E	R <sup>2</sup>
[Zn <sub>2</sub> (fum) <sub>2</sub> (bpy)]	0.478	−0.132	0.804	0.050	0.752	0.973	908	0.141	0.907	3.411	158	0.790
[Zn <sub>4</sub> O(bdc) <sub>3</sub> ]	47.62	0.012	0.174	0.208	0.760	0.993	365	0.209	0.976	10.78	223	0.957

Q<sub>max</sub>: maximum adsorption capacity; K<sub>L</sub>: Langmuir constant; K<sub>F</sub>: adsorption capacity for Freundlich model; n: intensity of the adsorption constant; B: constant related to heat sorption; A<sub>T</sub>: Temkin isotherm equilibrium binding constant; q<sub>s</sub>: theoretical isotherm saturation capacity; E: mean free energy; MOFs: metal–organic frameworks; bdc: benzene-1,4-dicarboxylate; bpy: 4,4-bipyridine; fum: fumaric acid.

mass of the adsorbent and finally decrease steadily after 0.03 g of the adsorbent have been used. The decrease in amodiaquine uptake with increasing adsorbent dosage as shown in Fig. 10 may be due to complex interactions of several factors which might be due to insufficient availability of the amodiaquine molecule to cover all the exchangeable sites on the MOFs at high adsorbent dosage, usually resulting to low amodiaquine uptake (Tangaromsuk et al., 2002; Selatnia et al., 2004). Also, aggregation of adsorbent particles at higher concentrations would lead to decrease in surface area and an increase in diffusion path length. The unsaturation of the adsorption sites during adsorption process might be another possibility (Gadd et al., 1988).

**2.3. Adsorption isotherms**

The equilibrium uptake data of amodiaquine on [Zn<sub>4</sub>O(bdc)<sub>3</sub>] and [Zn<sub>2</sub>(fum)<sub>2</sub>(bpy)] MOFs were analyzed using the Langmuir, Freundlich, Temkin, and Dubinin–Radushkevich isotherm models. The isotherm models are given in linear forms as:

$$\frac{C_{eq}}{q_{eq}} = \frac{1}{K_L \cdot q_{max}} + \frac{C_{eq}}{q_{max}} \text{ (Langmuir model)} \tag{2}$$

$$\log q_{eq} = \log K_F + \frac{1}{n} \log C_{eq} \text{ (Freundlich model)} \tag{3}$$

$$q_{eq} = B \ln A_T + B \ln C_{eq} \text{ (Temkin model)} \tag{4}$$

$$\ln q_{eq} = \ln (q_s) - (K_{ad} E^2) \text{ (Dubinin–Radushkevich model)} \tag{5}$$

where: q<sub>max</sub> is the maximum adsorption capacity (mg/g), q<sub>eq</sub> is the amount adsorbed per unit mass of the adsorbent at equilibrium (mg/g), C<sub>eq</sub> is the equilibrium concentration of adsorbate (mg/L), n is the intensity of the adsorption constant, K<sub>F</sub> (mg/g) is the adsorption capacity for Freundlich model, K<sub>L</sub> (L/mg) is Langmuir constant relating to adsorption strength or

intensity, A<sub>T</sub> is Temkin isotherm equilibrium binding constant (L/g), B is the constant related to heat sorption (J/mol), q<sub>s</sub> is the theoretical isotherm saturation capacity (mg/g), K<sub>ad</sub> is the Dubinin–Raduskevich isotherm constant, and E is the mean free energy (kJ/mol). Fig. 11 presents the linear plot of the Langmuir, Freundlich, Temkin, and Dubinin–Radushkevich isotherms respectively for the adsorption of amodiaquine on [Zn<sub>4</sub>O(bdc)<sub>3</sub>] and [Zn<sub>2</sub>(fum)<sub>2</sub>(bpy)] MOFs.

The theoretical parameters for the isotherms used in this study and their regression coefficient values are summarized in Table 2. The R<sup>2</sup> values indicate that Freundlich isotherm is the most suitable for this adsorption process. The Freundlich isotherm was observed to have the highest R<sup>2</sup> values of 0.973 and 0.993 for [Zn<sub>2</sub>(fum)<sub>2</sub>(bpy)] and [Zn<sub>4</sub>O(bdc)<sub>3</sub>] MOFs respectively. The fact that the Freundlich isotherm is the best fit isotherm for both MOFs implies that a multilayer adsorption occurred between the amodiaquine and the [Zn<sub>2</sub>(fum)<sub>2</sub>(bpy)] and [Zn<sub>4</sub>O(bdc)<sub>3</sub>] MOFs, which also indicates the heterogeneous nature of the MOFs involving physisorption (Njoku et al., 2014).

Although the Langmuir isotherm is not the best to be used in describing the adsorption process, the value of q<sub>max</sub> due to its theoretical background is usually used as the adsorption capacity (Wu et al., 2002). Therefore, the maximum adsorption capacities of the amodiaquine in this study were found to be 0.478 and 47.62 mg/g on the [Zn<sub>2</sub>(fum)<sub>2</sub>(bpy)] and [Zn<sub>4</sub>O(bdc)<sub>3</sub>] MOFs respectively.

As shown in Table 3, the adsorption capacity of [Zn<sub>4</sub>O(bdc)<sub>3</sub>] in this study is higher than other previous studies using MOFs or other adsorbent materials. This shows that [Zn<sub>4</sub>O(bdc)<sub>3</sub>] MOF is suitable for the removal of emerging contaminants, such as pharmaceuticals and personal care products from aqueous solution. However, there are other MOFs with higher adsorption capacity, for example MIL-100-Fe (Hasan et al., 2012), which has a higher adsorption capacity for naproxen.

**Table 3 – Adsorption capacities and mechanism of interaction of different adsorbents for pharmaceuticals and personal care products (PPCPs).**

Adsorbent	Adsorbate	Adsorption capacities (mg/g)	Mechanism of interaction	References
Zn <sub>2</sub> (fum) <sub>2</sub> (bpy)	Amodiaquine	0.478	Electrostatic interaction	This study
Zn <sub>4</sub> O(bdc) <sub>3</sub>	Amodiaquine	47.62	Electrostatic interaction	This study
Graphene nanoplatelets	Aspirin	13.02	π–π electron donor–acceptor interaction	Al-Khateeb et al., 2014
RGO-M	Ciprofloxacin	18.9	Electrostatic and π–π interaction	Tang et al., 2013
RGO-M	Norfloracin	23.3	Electrostatic and π–π interaction	Tang et al., 2013
MIL-100-Fe	Naproxen	115	Electrostatic interaction	Hasan et al., 2012

RGO-M: Reduced graphene oxide/magnetite composites; MIL-100-Fe: iron-benzenetricarboxylate.

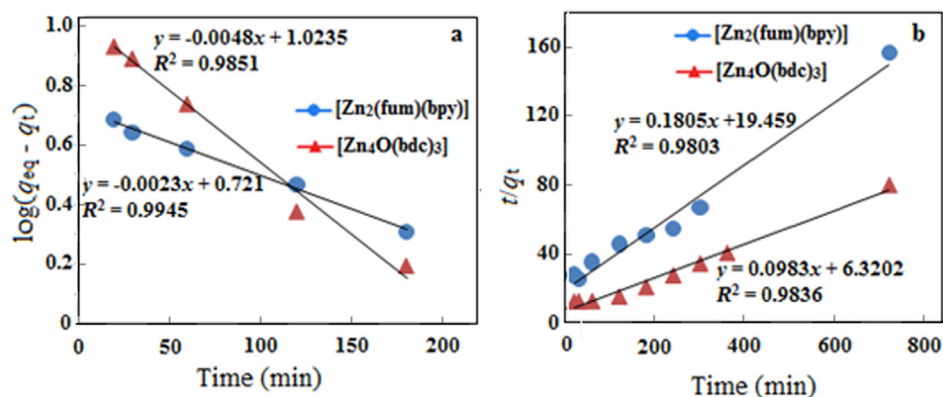


Fig. 12 – (a) Pseudo-first-order and (b) pseudo-second-order kinetic plot of amodiaquine.  $q_t$  and  $q_{eq}$  are the amounts of amodiaquine adsorbed per unit mass of the adsorbent (mg/g) at time  $t$ , and equilibrium, respectively.

#### 2.4. Adsorption kinetics

Linear plots of the pseudo-first-order and pseudo-second-order kinetic models were used to describe the adsorption kinetics of amodiaquine onto  $[Zn_2(\text{fum})_2(\text{bpy})]$  and  $[Zn_4O(\text{bdc})_3]$  MOFs and are presented in Fig. 12. The pseudo-first-order and pseudo-

second-order rate equations as reported previously by Elaigwu et al. (2014) are as follows:

$$\frac{1}{q_t} = \left(\frac{k_1}{q_{eq}}\right)\left(\frac{1}{t}\right) + \left(\frac{1}{q_{eq}}\right) \quad (6)$$

The pseudo-second-order rate equation is given by:

$$\frac{t}{q_t} = \frac{1}{k_2 q_{eq}^2} + \frac{t}{q_{eq}} \quad (7)$$

where:  $q_t$  and  $q_{eq}$  are the amounts of amodiaquine adsorbed per unit mass of the adsorbent (mg/g) at time,  $t$ , and equilibrium respectively;  $k_1$  is a pseudo-first-order kinetic constant expressed in  $\text{min}^{-1}$  and  $k_2$  is the pseudo-second-order rate constant given in  $\text{g}/\text{mg}/\text{min}$ .

The results of the pseudo-first-order and pseudo-second-order kinetics for this study show the correlation coefficient value ( $R^2$ ) for the pseudo-first-order to be higher than that of the pseudo-second-order (Table 4). This indicates that the experimental data obtained in this study fits better into the pseudo-first-order kinetic model.

Adsorbents	Pseudo-first-order		Pseudo-second-order	
	$k_1(\text{min}^{-1})$	$R^2$	$k_2(\text{g}/\text{mg}/\text{min})$	$R^2$
$[Zn_2(\text{fum})_2(\text{bpy})]$	0.00461	0.994	1.580	0.980
$[Zn_4O(\text{bdc})_3]$	0.00921	0.985	16.480	0.983

$k_1$ : pseudo-first-order rate constant;  $k_2$ : pseudo-second-order rate constant; bdc: benzene-1,4-dicarboxylate; bpy: 4,4'-bipyridine; fum: fumaric acid.

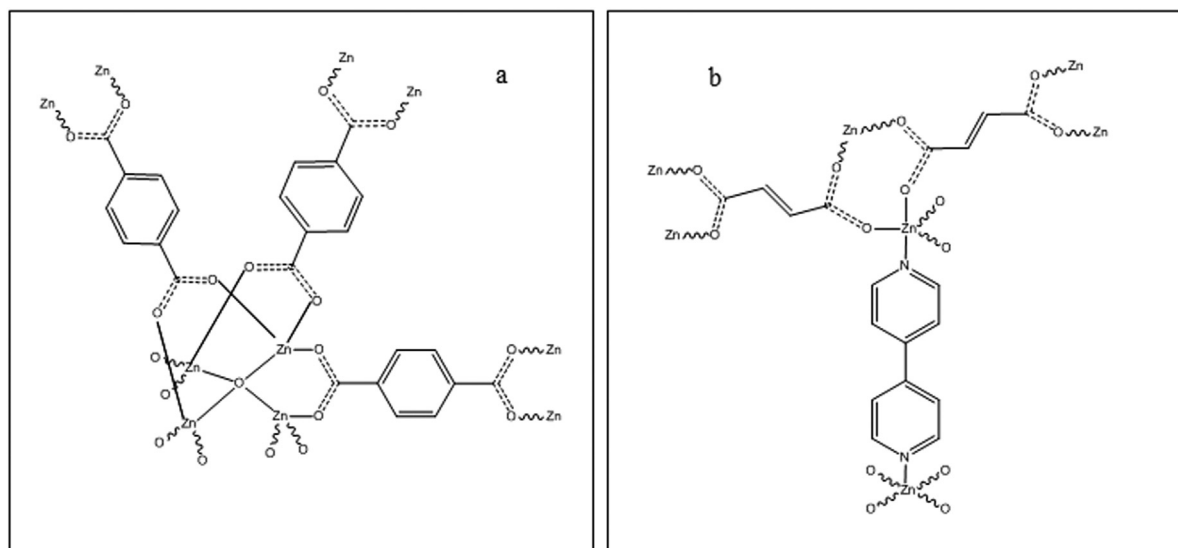


Fig. 13 – Structure of (a)  $[Zn_4O(\text{bdc})_3]$  (CCDC Refcode: SAHYIK; CCDC Number: 256965; Li et al., 1999; Eddaoudi et al., 1999) and (b)  $[Zn_2(\text{fum})_2(\text{bpy})]$  (CCDC Refcode: MAVNUT01; CCDC Number: 784694; Fujii et al., 2010).

### 2.5. Adsorption mechanism

The structures of the two MOFs are presented in Fig. 13. In the molecular unit of  $[Zn_4O(bdc)_3]$ , there are four different metal coordination sites to attract the negatively charged amodiaquine molecule whereas only one is present in  $[Zn_2(fum)_2(bpy)]$ . This account for the higher adsorption capacity of  $[Zn_4O(bdc)_3]$  compared to  $[Zn_2(fum)_2(bpy)]$ . The amodiaquine molecules are therefore adsorbed in four adsorption sites of  $Zn_4O$  clusters in  $[Zn_4O(bdc)_3]$ , but in  $[Zn_2(fum)_2(bpy)]$  amodiaquine molecules are absorbed only on one  $Zn^{2+}$  adsorption site. The mechanism of adsorption of amodiaquine on the two MOFs is therefore as a result of electrostatic interactions between the amodiaquine hydroxyl group ( $O^-$ ) and the  $Zn^{2+}$  metal centers.

### 3. Conclusions

$[Zn_2(fum)_2(bpy)]$  and  $[Zn_4O(bdc)_3]$  MOFs have been successfully prepared and used for the removal of amodiaquine from solution. The kinetics study results showed that the adsorption of amodiaquine over the  $[Zn_2(fum)_2(bpy)]$  and  $[Zn_4O(bdc)_3]$  MOFs followed the pseudo-first-order rate law and the Freundlich isotherm was found to be the most suitable to describe the adsorption process. Equilibrium was attained within 180 min and increase in temperature was observed to decrease the amount of amodiaquine adsorbed on the adsorbents. More amodiaquine was observed to be adsorbed over the  $[Zn_4O(bdc)_3]$  MOF compared to  $[Zn_2(fum)_2(bpy)]$  MOF. Results obtained in this study indicate that  $[Zn_4O(bdc)_3]$  MOF has the potential to be used as effective adsorbents for the removal of amodiaquine from aqueous solution.

### Acknowledgment

Adedibu C. Tella (ACT) and Samson O. Owalude (SOO) are grateful to the Royal Society of Chemistry for the award of 2016 Royal Society of Chemistry (RSC) Research Fund Grant.

### REFERENCES

- Abbasi, M., Saeed, F., Rafique, U., 2013. Preparation of silver nanoparticles from synthetic and natural sources: remediation model for PAHs. *Int. Symp. Adv. Mater. Mater. Sci. Eng.* 60, 012061.
- Ahmed, I., Bhadra, B.N., Lee, H.J., Jhung, S.H., 2017. Metal-organic framework-derived carbons: preparation from ZIF-8 and application in the adsorptive removal of sulfamethoxazole from water. *Catal. Today* <http://dx.doi.org/10.1016/j.cattod.2017.02.011>.
- Al-Khateeb, L.A., Almotiry, S., Salam, M.A., 2014. Adsorption of pharmaceutical pollutants onto graphene nanoplatelets. *Chem. Eng. J.* 248, 191–199.
- Arlinghaus, R.T., Andrews, L., 1984. Fourier-transform infrared spectra of alkyl halide/hydrogen fluoride hydrogen-bonded complexes in solid argon. *J. Phys. Chem.* 88, 4032–4036.
- Bajpai, S.K., Chand, N., Mahendra, M., 2014. The adsorptive removal of a cationic drug from aqueous solution using poly (methacrylic acid) hydrogels. *Water SA* 40, 1–9.
- Bhadra, B.N., Ahmed, I., Kim, S., Jhung, S.H., 2017. Adsorptive removal of ibuprofen and diclofenac from water using metal-organic framework-derived porous carbon. *Chem. Eng. J.* 314, 50–58.
- Boyd, G.R., Reemtsma, H., Grimm, D., Mitra, S.C., 2003. Pharmaceuticals and personal care products (PPCPs) in surface and treated waters of Louisiana, USA and Ontario, Canada. *Sci. Total Environ.* 311, 135–149.
- Boyd, G.R., Zhang, S., Grimm, D., 2005. Naproxen removal from water by chlorination and biofilm processes. *Water Res.* 39, 668–676.
- Chen, X., Chen, G., Chen, L., Chen, Y., Lehmann, J., McBride, M.B., Hay, A.G., 2011. Adsorption of copper and zinc by biochars produced from pyrolysis of hardwood and corn straw in aqueous solution. *Bioresour. Technol.* 102, 8877–8884.
- Chughtai, A.H., Ahmad, N., Younus, H.A., Laypkov, A., Verpoort, F., 2015. Metal-organic frameworks: versatile heterogeneous catalysts for efficient catalytic organic transformations. *Chem. Soc. Rev.* 44, 6804–6849.
- Corma, A., García, H., Llabrésixamena, F.X., 2010. Engineering metal organic frameworks for heterogeneous catalysis. *Chem. Rev.* 110, 4606–4655.
- Cuerda-Correa, E.M., Dominguez-Vargas, J.R., Olivares-Marin, F.J., Heredia, J.B., 2010. On the use of carbon blacks as potential low-cost adsorbents for the removal of non-steroidal anti-inflammatory drugs from river water. *J. Hazard. Mater.* 177, 1046–1053.
- Dikio, E.D., Farah, A.M., 2013. Synthesis, characterization and comparative study of copper and zinc metal organic frameworks. *Chem. Sci. Trans.* 2, 1386–1394.
- Eddaoudi, M., Li, H., Reineke, T., Fehr, M., Kelley, D., Groy, T.L., Yaghi, O.M., 1999. Design and synthesis of metal-carboxylate frameworks with permanent microporosity. *Top. Catal.* 9, 105–111.
- Elaiwu, S.E., Rocher, V., Kyriakou, G., Greenway, G.M., 2014. Removal of  $Pb^{2+}$  and  $Cd^{2+}$  from aqueous solution using chars from pyrolysis and microwave-assisted hydrothermal carbonization of *Prosopis Africana* shell. *J. Ind. Eng. Chem.* 20, 3467–3473.
- Ereira, V.J., Lindane, K.G., Weinberg, H.S., 2007. Evaluation of UV irradiation for photolytic and oxidative degradation of pharmaceutical compounds in water. *Water Res.* 41, 4413–4423.
- Eren, Z., Acar, F.N., 2006. Adsorption of reactive black 5 from an aqueous solution: equilibrium and kinetic studies. *Desalination* 194, 1–3.
- Ernes, T.A., Stuber, J., Herrmann, N., McDowel, L.D., Ried, A., Kampmann, M., Teiser, B., 2003. Ozonation: a tool for removal of pharmaceuticals, contrast media and musk fragrances from wastewater? *Water Res.* 37, 1976–1982.
- Fan, L., Yan, X.P., 2012. Evaluation of isostructural metal-organic frameworks coated capillary columns for the gas chromatographic separation of alkane isomers. *Talanta* 99, 944–950.
- Fehintola, F.A., Akinyinka, O.O., Adewole, I.F., 2011. Drug interactions in the treatment and chemoprophylaxis of malaria in HIV infected individuals in sub Saharan Africa. *Curr. Drug Metab.* 12, 51–56.
- Fujii, K., Garay, A.L., Hill, J., Sbircea, E., Pan, Z., Xu, M., Apperley, D.C., James, S.L., Harris, K.D.M., 2010. Direct structure elucidation by powder X-ray diffraction of a metal-organic framework material prepared by solvent-free grinding. *Chem. Commun.* 46, 7572–7574.
- Gadd, G.M., White, C., de Rome, L., 1988. Heavy metal and radionuclide uptake by fungi and yeasts. In: Norris, P.R., Kelly, D.P. (Eds.), *Biohydrometallurgy, Proceedings of the International Symposium, Warwick, 1987*. Science and Technology Letters, Kew, Surrey, pp. 421–435.
- Getman, R.B., Bae, Y.S., Wilmer, C.E., Snurr, R.Q., 2011. Review and analysis of molecular simulations of methane, hydrogen, and

- acetylene storage in metal-organic frameworks. *Chem. Rev.* 112, 703–723.
- Hasan, Z., Jeon, J., Jhung, S.H., 2012. Adsorptive removal of naproxen and clofibrac acid from water using metal-organic frameworks. *J. Hazard. Mater.* 209–210, 151–157.
- Hodel, E.M., Genton, B., Zanolari, B., Mercier, T., Duong, S., Beck, H.P., Olliaro, P., Decosterd, L.A., Ariey, F., 2010. Residual antimalarial concentrations before treatment in patients with malaria from Cambodia: indication of drug pressure. *J. Infect. Dis.* 202, 1088–1094.
- Huang, C.Y., Song, M., Gu, Z.Y., Wang, H.F., Yan, X.P., 2011. Probing the adsorption characteristic of metal-organic framework MIL-101 for volatile organic compounds by quartz crystal microbalance. *Environ. Sci. Technol.* 45, 4490–4494.
- Ibrahim, M., Nada, A., Kamal, D.E., 2005. Density functional theory and FTIR spectroscopic study of carboxyl group. *Indian J. Pure Appl. Phys.* 43, 911–917.
- Isaeva, V.I., Tkachenko, O.P., Mishin, I.V., Kapustin, G.I., Kostin, A.A., Klementiev, K.V., Kustov, L.M., 2008. Application of MOF-5 as a component of heterogeneous catalytic systems for the liquid phase hydrogenation. *Stud. Surf. Sci. Catal. A* 174, 463–466.
- Kannan, N., Sundaram, M.M., 2001. Kinetics and mechanism of removal of methylene blue by adsorption on various carbons—a comparative study. *Dyes Pigments* 51, 25–40.
- Karunajeewa, H.A., 2015. Parasite clearance after malaria therapy: staying a step ahead of drug resistance. *BMC Med.* 13, 1–4.
- Khan, M.N., Sarwar, A., 2007. Determination of point of zero charge of natural and treated adsorbents. *Surf. Rev. Lett.* 14, 461–469.
- Kleist, W., Maciejewski, M., Baiker, A., 2010. MOF-5 based mixed-linker metal-organic frameworks: synthesis, thermal stability and catalytic application. *Thermochim. Acta* 499, 71–78.
- Kopel, E., Marhoom, E., Sidi, Y., Schwartz, E., 2012. Successful oral therapy for severe *falciparum* malaria: the World Health Organization criteria revisited. *Am. J. Trop. Med. Hyg.* 86, 409–411.
- Koram, K.A., Abuaku, B., Duah, N., Quashie, N., 2005. Comparative efficacy of antimalarial drugs including ACTs in the treatment of uncomplicated malaria among children under 5 years in Ghana. *Acta Trop.* 95, 194–203.
- Koram, K.A., Quaye, L., Abuaku, B., 2008. Efficacy of amodiaquine/artesunate combination therapy for uncomplicated malaria in children under five years in Ghana. *Ghana Med. J.* 42, 55–60.
- Korenromp, E.L., Hosseini, M., Newman, R.D., Cibulskis, R.E., 2013. Progress towards malaria control targets in relation to national malaria programme funding. *Malar. J.* 12, 1–9.
- Koyuncu, O.A., Arikan, M., Wiesner, R., Rice, C., 2008. Removal of hormones and antibiotics by nanofiltration membranes. *J. Membr. Sci.* 309, 94–101.
- Li, H., Eddaoudi, M., O’Keeffe, M., Yaghi, O.M., 1999. Synthesis of an exceptionally stable and highly porous metal-organic framework. *Nature* 402, 276–279.
- Li, J., Cheng, S., Zhao, Q., Long, P., Dong, J., 2009. Synthesis and hydrogen-storage behavior of metal-organic framework MOF-5. *Int. J. Hydrogen Energy* 34, 1377–1382.
- Li, Z., Hong, H., Liao, L., Ackley, C.J., Schulz, L.A., MacDonald, R.A., Mihelich, A.L., Emard, S.M., 2011. A mechanistic study of ciprofloxacin removal by kaolinite. *Colloids Surf. B: Biointerfaces* 88, 339–344.
- Li, J.R., Sculley, J., Zhou, H.C., 2012. Metal-organic frameworks for separations. *Chem. Rev.* 112, 869–932.
- Liu, J.-Q., Li, X.-F., Gu, C.-Y., da Silva, J.C.S., Barros, A.L., Alves-Jr, S., Li, B.-H., Ren, F., Battene, S.R., Soares, T.A., 2015. A combined experimental and computational study of novel nanocage-based metal-organic frameworks for drug delivery. *Dalton Trans.* 44, 19370–19382.
- Liu, J.-Q., Wu, J., Li, F.-M., Liu, W.-C., Li, B.-H., Wang, J., Li, Q.-L., Yadav, R., Kumar, A., 2016a. Luminescent sensing from a new Zn(II) metal-organic framework. *RSC Adv.* 6, 31161–31166.
- Liu, J., Liu, G., Gu, C., Liu, W., Xu, J., Li, B., Wang, W., 2016b. Rational synthesis of a novel 3,3,5-c polyhedral metal-organic framework with high thermal stability and hydrogen storage capability. *J. Mater. Chem. A* 4, 11630–11634.
- Luo, J., Wang, J., Li, G., Huo, Q., Liu, Y., 2013. Assembly of a unique octa-nuclear copper cluster-based metal-organic framework with highly selective CO<sub>2</sub> adsorption over N<sub>2</sub> and CH<sub>4</sub>. *Chem. Commun.* 49, 11433–11435.
- Ma, D.-Y., Li, Z., Xiao, J.-X., Deng, R., Lin, P.-F., Chen, R.-Q., Liang, Y.-Q., Guo, H.-F., Liu, B., Liu, J.-Q., 2015. Hydrostable and nitril/methyl-functionalized metal-organic framework for drug delivery and highly selective CO<sub>2</sub> adsorption. *Inorg. Chem.* 54, 6719–6726.
- Ma, J., Yao, Z., Hou, L., Lu, W., Yang, Q., Li, J., Chen, L., 2016. Metal organic frameworks (MOFs) for magnetic solid-phase extraction of pyrazole/pyrrole pesticides in environmental water samples followed by HPLC-DAD determination. *Talanta* 161, 686–692.
- Marin, F.J., Beltran, D.E., Heredia, J., 2010. On the use of carbon blacks as potential low-cost adsorbents for the removal of non-steroidal anti-inflammatory drugs from river water. *J. Hazard. Mater.* 177, 1046–1053.
- Nikolaou, A., Meric, S., Fatta, D., 2007. Occurrence patterns of pharmaceuticals in water and wastewater environments. *Anal. Bioanal. Chem.* 387, 1225–1234.
- Njoku, V.O., Islam, M.A., Asif, M., Hameed, B.H., 2014. Utilization of sky fruit husk agricultural waste to produce high quality activated carbon for the herbicide bentazon adsorption. *Chem. Eng. J.* 251, 183–191.
- Olgun, A., Atar, N., 2012. Equilibrium, thermodynamic and kinetic studies for the adsorption of lead (II) and nickel (II) onto clay mixture containing boron impurity. *J. Ind. Eng. Chem.* 18, 1751–1757.
- Phan, N.T., Le, K.A., Phan, T.D., 2010. MOF-5 as an efficient heterogeneous catalyst for Friedel-Crafts alkylation reactions. *Appl. Catal. A* 382, 246–253.
- Rasheed, N.M., 2013. Adsorption technique for the removal of organic pollutants from water and wastewater. In: Rasheed, N.M. (Ed.), *Organic Pollutants – Monitoring, Risk and Treatment*. Intech, Rijeka, pp. 167–194.
- Rowell, J.L.C., Yaghi, O.M., 2004. Metal-organic frameworks: a new class of porous materials. *Microporous Mesoporous Mater.* 73, 3–14.
- Rowell, J.L.C., Milward, A.R., Park, K.S., Yaghi, O.M., 2004. Hydrogen sorption in functionalized metal-organic frameworks. *J. Am. Chem. Soc.* 126, 5666–5667.
- Selatnia, A., Boukazoula, A., Kechid, N., Bakhti, M.Z., Chergui, A., Kerchich, Y., 2004. Biosorption of lead(II) from aqueous solution by a bacterial dead *Streptomyces rimosus* biomass. *Biochem. Eng. J.* 19, 127–135.
- Seo, P.W., Bhadra, B.N., Ahmed, I., Khan, N.A., Jhung, S.H., 2016. Adsorptive removal of pharmaceuticals and personal care products from water with functionalized metal-organic frameworks: remarkable adsorbents with hydrogen bonding abilities. *Sci Rep* 6, 34462.
- Seo, P.W., Khan, N.A., Jhung, S.H., 2017. Removal of nitroimidazole antibiotics from water by adsorption over metal-organic frameworks modified with urea or melamine. *Chem. Eng. J.* 315, 92–100.
- Tang, Y., Guo, H., Xiao, L., Yu, S., Gao, N., Wang, Y., 2013. Synthesis of reduced graphene oxide/magnetite composites and investigation of their adsorption performance of fluoroquinolone antibiotics. *Colloids Surf. A: Physicochem. Eng. Aspect* 424, 74–80.
- Tangaromsuk, J., Pokethitiyook, P., Kruatrachue, M., Utham, E.S., 2002. Cadmium biosorption by *Sphingomonas paucimobilis* biomass. *Bioresour. Technol.* 85, 103–105.

- Taylor-Pashow, K.M.L., Rocca, J.D., Xie, Z., Tran, S., Lin, S.W., 2009. Post-synthetic modifications of iron-carboxylate nanoscale metal-organic frameworks for imaging and drug delivery. *J. Am. Chem. Soc.* 131, 14261–14263.
- Tella, A.C., Owalude, S.O., 2014. A green route approach in the synthesis of Ni(II) and Zn(II) templated metal-organic frameworks. *J. Mater. Sci.* 49, 5635–5639.
- Tella, A.C., Owalude, S.O., Ojekanmi, C.A., Oluwafemi, S.O., 2014. Synthesis of copper-isonicotinate metal-organic frameworks simply by mixing solid reactants and investigation of their adsorptive properties for the removal of the fluorescein dye. *New J. Chem.* 38, 4494–4500.
- Wen, Y., Chen, L., Li, J., Liu, D., Chen, L., 2014. Recent advances in solid-phase sorbents for sample preparation prior to chromatographic analysis. *TrAC Anal. Chem.* 59, 26–41.
- Wittes, R., 1987. Adverse reactions to chloroquine and amodiaquine as used for malaria prophylaxis: a review of the literature. *Can. Fam. Physician* 33, 2644–2649.
- Wolfová, R., Pertile, E., Feč, P., 2013. Removal of lead from aqueous solution by walnut shell. *J. Environ. Chem. Ecotoxicol.* 5, 159–167.
- Wu, F.-C., Tseng, R.-L., Juang, R.-S., 2002. Adsorption of dyes and humic acid from water using chitosan-encapsulated activated carbon. *J. Chem. Technol. Biotechnol.* 77, 1269–1279.
- Xie, S.M., Zhang, Z.J., Wang, Z.Y., Yuan, L.M., 2011. Chiral metal-organic frameworks for high-resolution gas chromatographic separations. *J. Am. Chem. Soc.* 133, 11892–11895.
- Yaghi, O.M., O’Keeffe, M., Ockwig, N.W., Chae, H.K., Eddaoudi, M., Kim, J., 2003. Reticular synthesis and the design of new materials. *Nature* 423, 705–714.
- Zhang, X., Gao, X., Huo, P., Yan, Y., 2012. Selective adsorption of micro ciprofloxacin by molecularly imprinted functionalized polymers appended onto ZnS. *Environ. Technol.* 33, 2019–2025.